Evidence for the spin-orbit-induced $p^4(^1D_2)md\ ^2F^e$ resonances in atomic Br and Cl

S. Benzaid,[1] A. Menzel,[1] J. Jiménez-Mier,[2] S. J. Schaphorst,[1] M. O. Krause,[1] and C. D. Caldwell[1]
[1]*Department of Physics, University of Central Florida, Orlando, Florida 32816-2385*
[2]*Instituto de Ciencias Nucleares, Universidad Nacional Autonoma de México, 04510 México, Distrito Federal, Mexico*
(Received 29 April 1996)

Evidence is presented for the occurrence of the *LS*-forbidden $p^4(^1D_2)md\,^2F^e$ autoionization resonances in both Br and Cl by a measurement of the photoelectrons associated with the *J*-resolved $^3P_{2,1,0}$ final ionic states. Effects of spin-orbit coupling are delineated at the *J*-term level for both the $^2F^e$ and the $^2S^e$ resonances, and differences for these spin-orbit-induced pathways are highlighted. [S1050-2947(96)50510-X]

PACS number(s): 32.80.Dz, 32.80.Fb

While excitation of the $p^4(^1D_2)md\,^2F^e$ resonances between the $^3P_0$ and $^1D_2$ ionization thresholds of the halogen atoms is forbidden in *LS* coupling, a weak feature has been predicted by theory to occur in Cl [1] and Br [2] if spin-orbit coupling is taken into account. However, no such features could be discerned in the early absorption spectra [3,4] or the pioneering ion-yield measurements of Ruscić and Berkowitz on the autoionizing $(^1D_2)md,ns$ series in Cl [5] and Br [6]. We report here unambiguous experimental evidence for the existence of the $^2F^e$ excitations, obtained in a photoelectron spectrometry experiment in which the $X^*p^4(^1D_2)md,ns(^2S,^2P,^2D,^2F)$ resonance states in the halogen atom *X* excited from the $Xp^5(^2P^o_{3/2})$ ground state are distinguished at the *J* level of the $X^+p^4(^3P_J)\epsilon\ell$ exit channels. Spin-orbit coupling also accounts for the decay of the $p^4(^1D_2)md(^2S)$ resonances into the $X^+p^4(^3P)$ channels, as has been recognized in earlier work [1,2,6]. However, the two pathways exhibit important differences. In the two-step approach to autoionization, it is the *excitation* of $^2F^e$ that depends on spin-orbit coupling, with the decay being allowed in *LS* coupling; while the excitation of $^2S^e$ is *LS* allowed, with the *decay* being spin-orbit induced. The *J*-level differentiation achieved in this experiment has allowed us to delineate these differences.

The experiment was performed at the 4-m normal-incidence monochromator (NIM) of the University of Wisconsin Synchrotron Radiation Center. Operational procedures for our electron spectrometer and the microwave-driven discharge tube serving as the source of the halogen atoms were similar to those used in previous experiments [7,8]. For the present experiment the monochromator was set to a bandpass of 16 pm (full width at half maximum), and the electron spectrometer to a resolution of about 50 meV. The discharge was operated at low power to optimize the stability of the atomic source and the signal-to-noise ratio. The autoionization region was studied in the constant-ionic-state (CIS) mode, in which the energy of an electron associated with a particular $X^+(^3P_J)$ state and the photon energy are scanned simultaneously, thus uniquely defining the final ionic state at the *J* level. Both partial and differential cross sections were measured on a relative basis over the first three $md,ns(^2S,^2P,^2D,^2F)$ groups of the Beutler-Fano-type resonances converging to the $^1D_2$ threshold.

Figures 1 and 2 show the photoelectron spectra of the $X^+(^3P_J)$ multiplets for Br and Cl, respectively, as recorded within the range of the resonance groups selected. In Br all *J* components are seen to be cleanly separated. In Cl the *J* components are sufficiently resolved to allow CIS measurements over the $J=2$ and $J=1$ components. The bromine spectrum is used, following a transmission correction for the electron-energy analyzers, to normalize the *J*-resolved CIS spectra, shown in Fig. 3, to each other.

The autoionization features of the second resonance group in Br, comprising the $Br^*4p^4(^1D_2)6d\ (^2P,^2D,^2S,^2F)$ and $Br^*4p^4(^1D_2)8s(^2D)$ members, are presented in Fig. 3 for all *J* components and their sum, which is equivalent to the (relative) absorption or ion-yield cross section. All spectra clearly exhibit the $6d(^2F)$ resonance at 12.712(2) eV. The resonance has a width of about 6 meV and appears as a relatively weak window in the $^3P_2$ channel, a dispersive resonance in $^3P_1$, and a strongly dispersive resonance in $^3P_0$. The resonance is surprisingly strong in the $^3P_0$ channel when compared with the broad $6d(^2P,^2D)$ feature. The shape and relative strength of ^2F in the total (sum) cross section are in general accord with the prediction by Robicheaux and Greene [2], as is, indeed, the overall structure of the resonance group. As expected on the basis of a weak spin-orbit interaction, the ^2F resonance in Cl is very weak and can only be seen in the $^3P_1$ channel at the present level of experimentation. It is most pronounced in the differential $^3P_1$ cross section at 0° (measured with respect to the

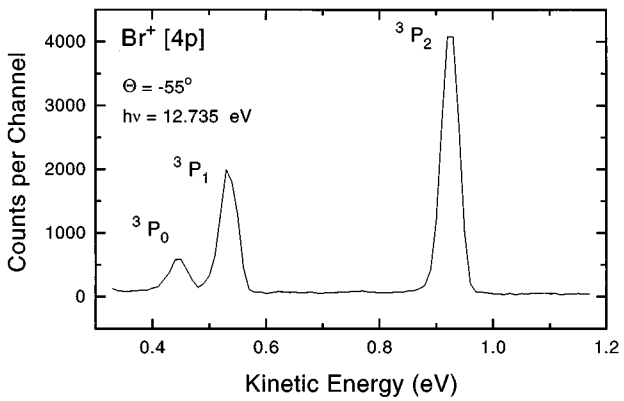

FIG. 1. Photoelectron spectrum of the $Br^+{}^3P_J$ multiplet at $h\nu=12.735$ eV, within the $4p^4(^1D_2)6d,8s$ resonance group, as recorded.

 © 1996 The American Physical Society

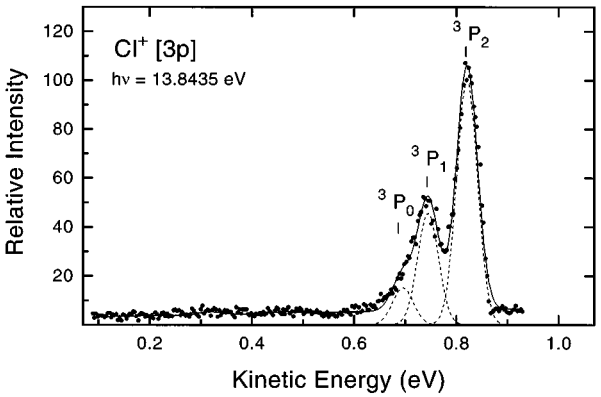

FIG. 2. Photoelectron spectrum of the $Cl^{+3}P_J$ multiplet at $h\nu = 13.8435$ eV, within the $3p^4(^1D_2)5d,7s$ resonance group.

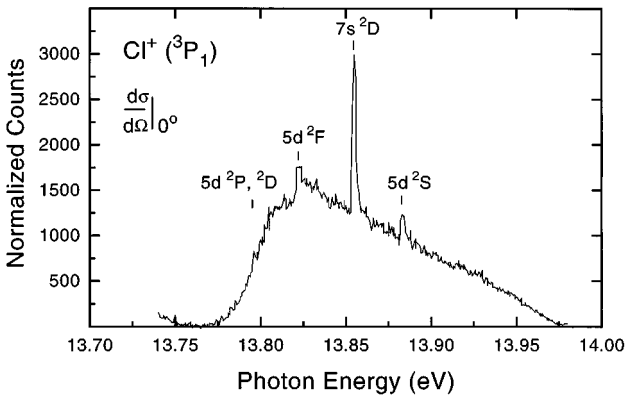

FIG. 4. Differential cross section at $\Theta = 0°$ in the $Cl^{+3}P_1$ channel across the $3p^4(^1D_2)5d,7s(^2P,^2D,^2F,^2S)$ autoionization resonances. The bandpass is 2.5 meV; the stepsize is 0.5 meV.

photon polarization axis), as illustrated in Fig. 4. The shape of the ^2F resonance shown in the figure resembles the shape of the analogous feature in Br at the same angle. Considering the regularities noted for the various properties of the halogen autoionization features [2], this resemblance is not surprising. The loci of the $md(^2F)$ resonances near the maxima of the corresponding $md(^2P,^2D)$ broad resonances are at variance with the prediction [1], but the energy of 13.463(2) eV for $4d(^2F)$ is in good accord with the theoretical value of 13.470 eV given by Hansen *et al.* [1].

The differing role of the spin-orbit interaction for the ^2F and ^2S resonances leads to profound differences in the autoionization spectra. Since the ^2F intermediate state is allowed in LS coupling to decay into all $^3P_{0,1,2}$ continua, it

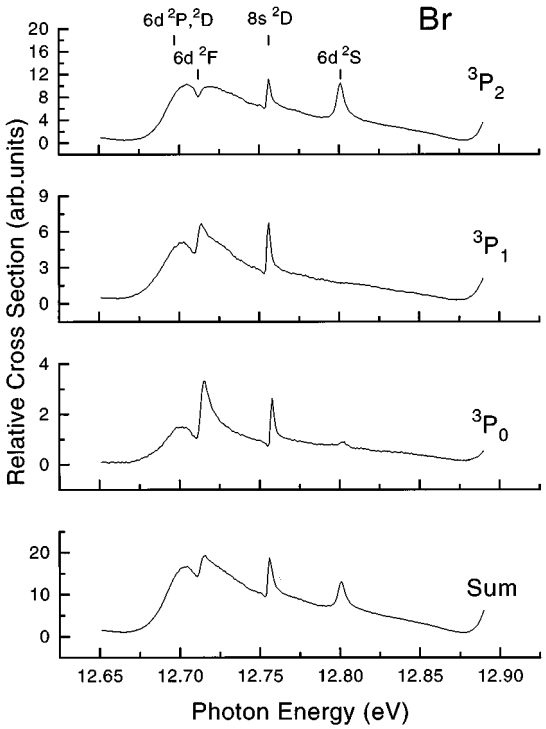

FIG. 3. Partial and total cross sections for the $Br^{+3}P_J$ components across the $4p^4(^1D_2)6d,8s(^2P,^2D,^2F,^2S)$ autoionization resonances. The spectra are normalized to each other. The bandpass is 2 meV; the stepsize is 1.0 meV.

can readily populate all exit channels, which is in accordance with observation (cf. Fig. 3). By contrast, while excitation of the ^2S intermediate state is allowed in LS coupling, its decay requires spin-orbit interactions. Hence, the decay will depend on the particular interactions available and may be influenced strongly. As Fig. 3 shows for Br, a strong discrimination according to the J value of the ^3P_J channel does indeed occur. Virtually the entire decay strength is seen to be in the $^3P_2$ channel. This is consistent with the expectation [1,2] that the decay of the $(^1D_2)md\,^2S$ state into the $^3P_2$ continuum channel is induced by the coupling of the $^1D_2$ and $^3P_2$ ''core'' states. The weak interference structure observed in the $^3P_0$ channel, and a barely identifiable excursion in the $^3P_1$ channel, are probably induced by more complex interchannel interactions. In the case of Cl, the predominant decay route from ^2S is also to the $^3P_2$ continuum channel, but there remains a definite, albeit small, signal in the $^3P_1$ channel. We cannot ascertain whether this signal is in part due to a residual overlap with the $^3P_2$ and $^3P_0$ peaks and in part due to relatively stronger interchannel interaction than in Br.

In conclusion, we have obtained evidence for the hitherto unobserved spin-orbit-induced $p^4(^1D_2)md(^2F^e)$ resonances in the autoionization series converging to the $^1D_2$ ionization threshold in both Br and Cl. The differentiation of the autoionization processes by the fine structure allowed us to delineate the consequences of spin-orbit coupling in the $^3P_2$, $^3P_1$, and $^3P_0$ partial cross sections and highlight the differences between the LS-forbidden ^2F and ^2S autoionization dynamics. The results of this work demonstrate the influence of spin-orbit coupling on the autoionization process in the halogen atoms. The results may provide a useful basis for the phenomenon in other open-shell atoms and can provide a gauge for theoretical calculations yet to be undertaken explicitly at the fine-structure level resolved in this study. A full analysis of our data, which include the energies, widths, shape parameters, and photoelectron angular distribution parameters for all series in both Cl [9] and Br [10], is planned in the near future.

This work is supported by NSF Grant No. PHY-9507573. The loan of equipment by the Oak Ridge National Laboratory is gratefully acknowledged. The SRC is supported under NSF Grant No. DMR-9531009.

[1] J.E. Hansen, R.D. Cowan, S.L. Carter, and H.P. Kelly, Phys. Rev. A **30**, 1540 (1984).
[2] F. Robicheaux and C.H. Greene, Phys. Rev. A **46**, 3821 (1992).
[3] R.E. Huffman, J.C. Larrabee, and Y. Tanaka, J. Chem. Phys. **47**, 856 (1967).
[4] V.N. Sarma and Y.N. Joshi, J. Phys. B **16**, 1671 (1983).
[5] B. Ruscić and J. Berkowitz, Phys. Rev. Lett. **50**, 675 (1983).
[6] B. Ruscić, J.P. Greene, and J. Berkowitz, J. Phys. B **17**, 1503 (1984).
[7] P. van der Meulen, M.O. Krause, and C.A. DeLange, J. Phys. B **25**, 97 (1992).
[8] C.D. Caldwell and M.O. Krause, J. Phys. B **27**, 4891 (1994).
[9] J. Jiménez-Mier, S.J. Schaphorst, C.D. Caldwell, and M.O. Krause (unpublished).
[10] S. Benzaid, A. Menzel, M.O. Krause, and C.D. Caldwell (unpublished).